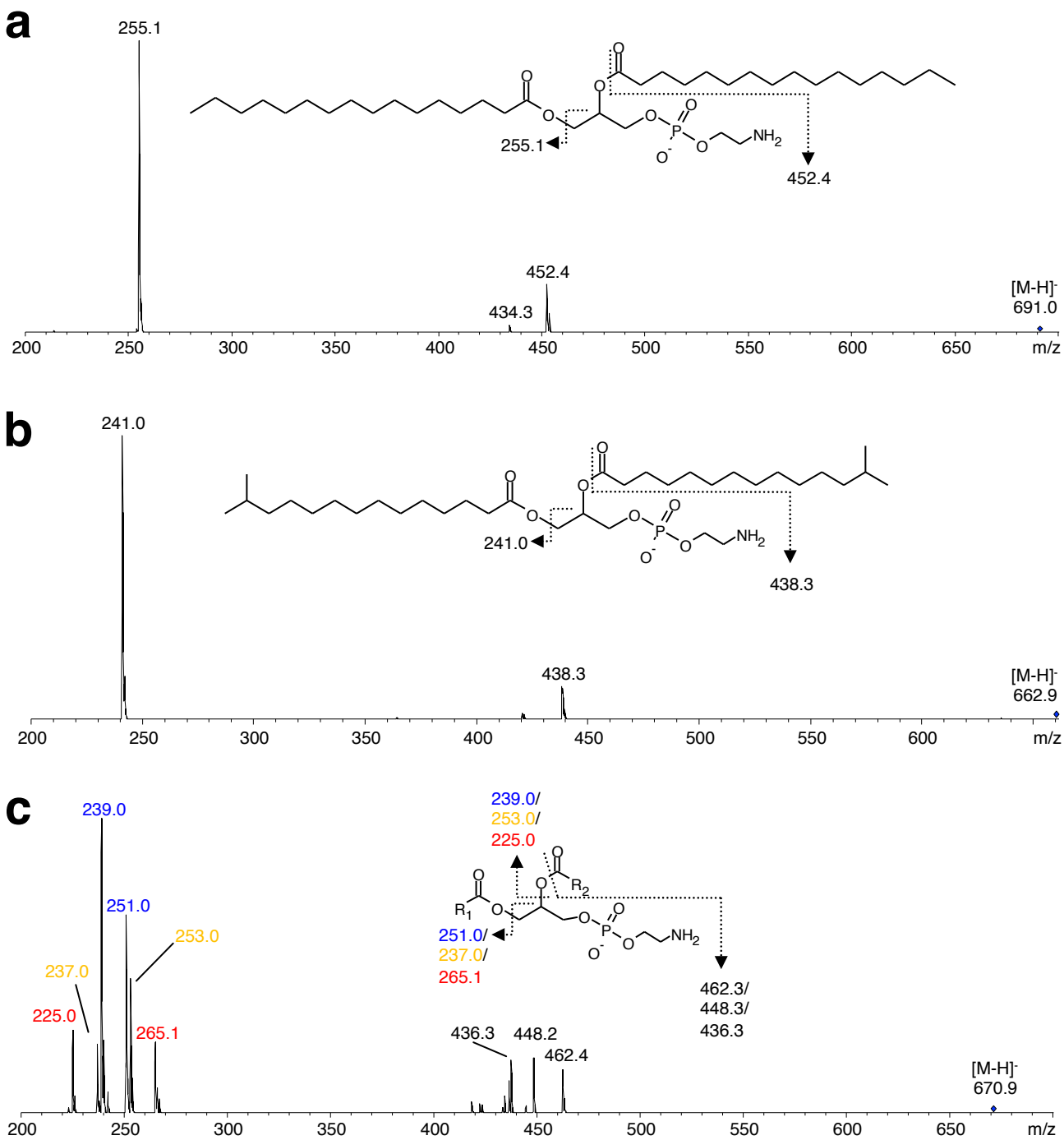

Supplementary Figure 1 | Example spectra for glycerophosphoethanolamine (PE) identification. Mass spectra of **a)** PE(16:0/16:0) lipid standard **b)** PE(15:0/15:0), the main glycerophosphoethanolamine in *M. xanthus*, and **c)** combined PE(16:2/15:1) (blue); PE(15:2/16:1) (orange); PE(17:2/14:1) (red) spectrum. Fragment signals derive from $[RCOO_{sn\text{-}1}]^-$ / $[RCOO_{sn\text{-}2}]^-$ as well as $[M\text{-}H\text{-}RCHO]^-$ and $[M\text{-}H\text{-}RCHO\text{-}H_2O]^-$ (not assigned) ions (27). Carboxylate ions with the higher relative abundance were assigned to the *sn*-2 position of the glycerol backbone (31).

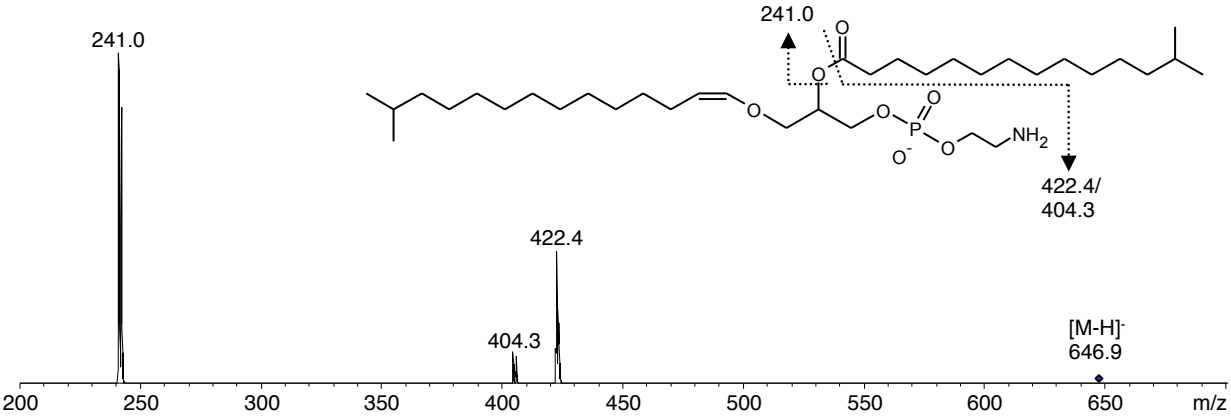

Supplementary Figure 2 | Example spectrum for 1*Z*-alkenylglycerophosphoethanolamine (PE(P)) identification. Mass spectrum of PE(P-15:0/15:0). Fragment signals derive from $[RCOO_{sn-2}]^-$ as well as $[M-H-RCHO]^-$ and $[M-H-RCHO-H_2O]^-$ ions (4).

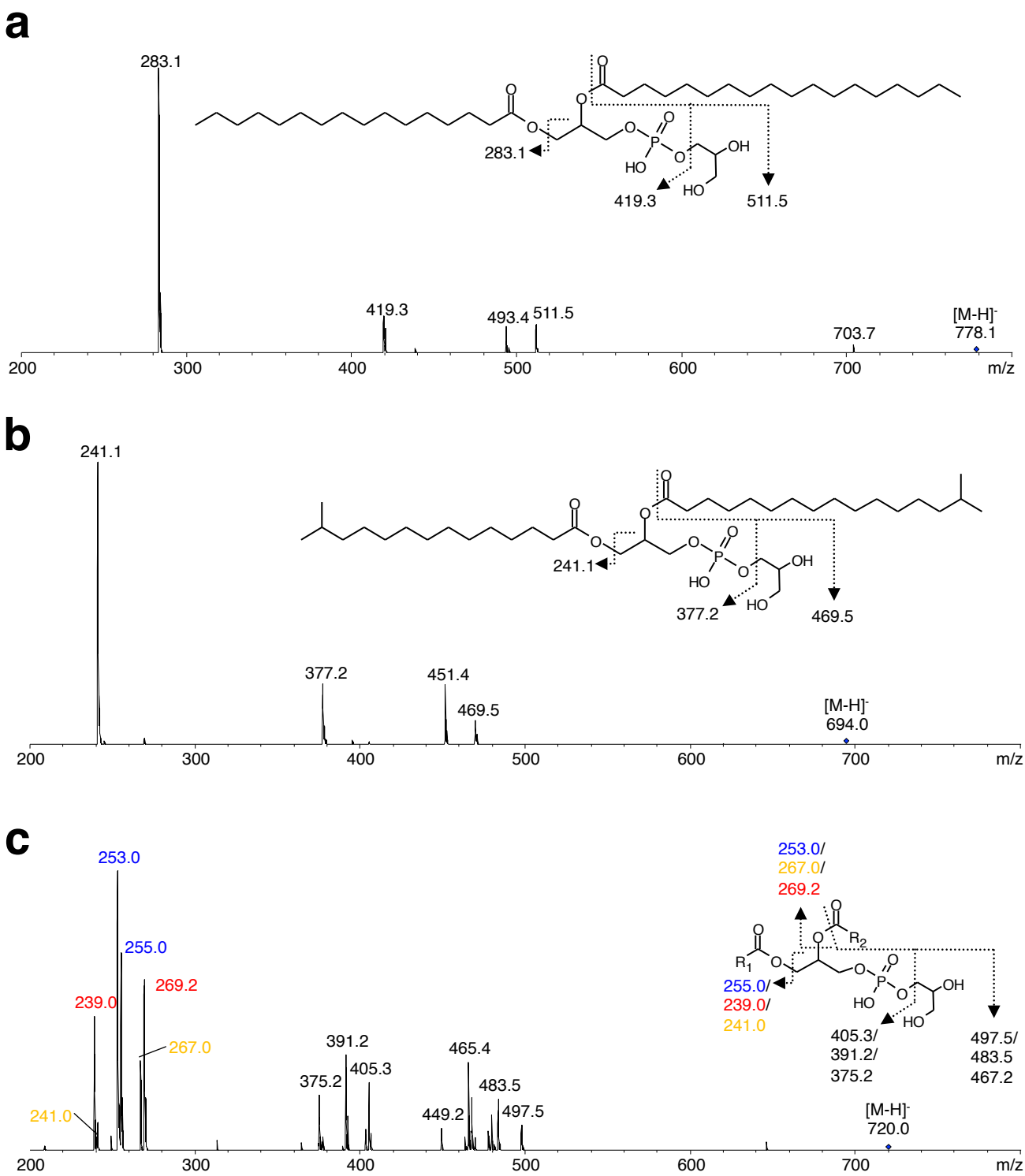

Supplementary Figure 3 | Example spectra for glycerophosphoglycerol (PG) identification. Mass spectra of **a)** PG(18:0/18:0) lipid standard **b)** PG(15:0/15:0), the main glycerophosphoglycerol in *M. xanthus*. and **c)** combined PG(16:0/16:1) (blue); PG(15:1/17:0) (red); PG(15:0/17:1) (orange) spectrum**.** Signals derive from $[RCOO_{sn\text{-}1}]^-$ / $[RCOO_{sn\text{-}2}]^-$ ions as well as $[M–H–74–RCH_2COOH]^-$, $[M\text{-}H\text{-}RCHO]^-$/$[M\text{-}H\text{-}RCHO\text{-}H_2O]^-$ (the latter not assigned) (32). Caboxylate ions with the higher relative abundance were assigned to the *sn*-2 position of the glycerol backbone (31).

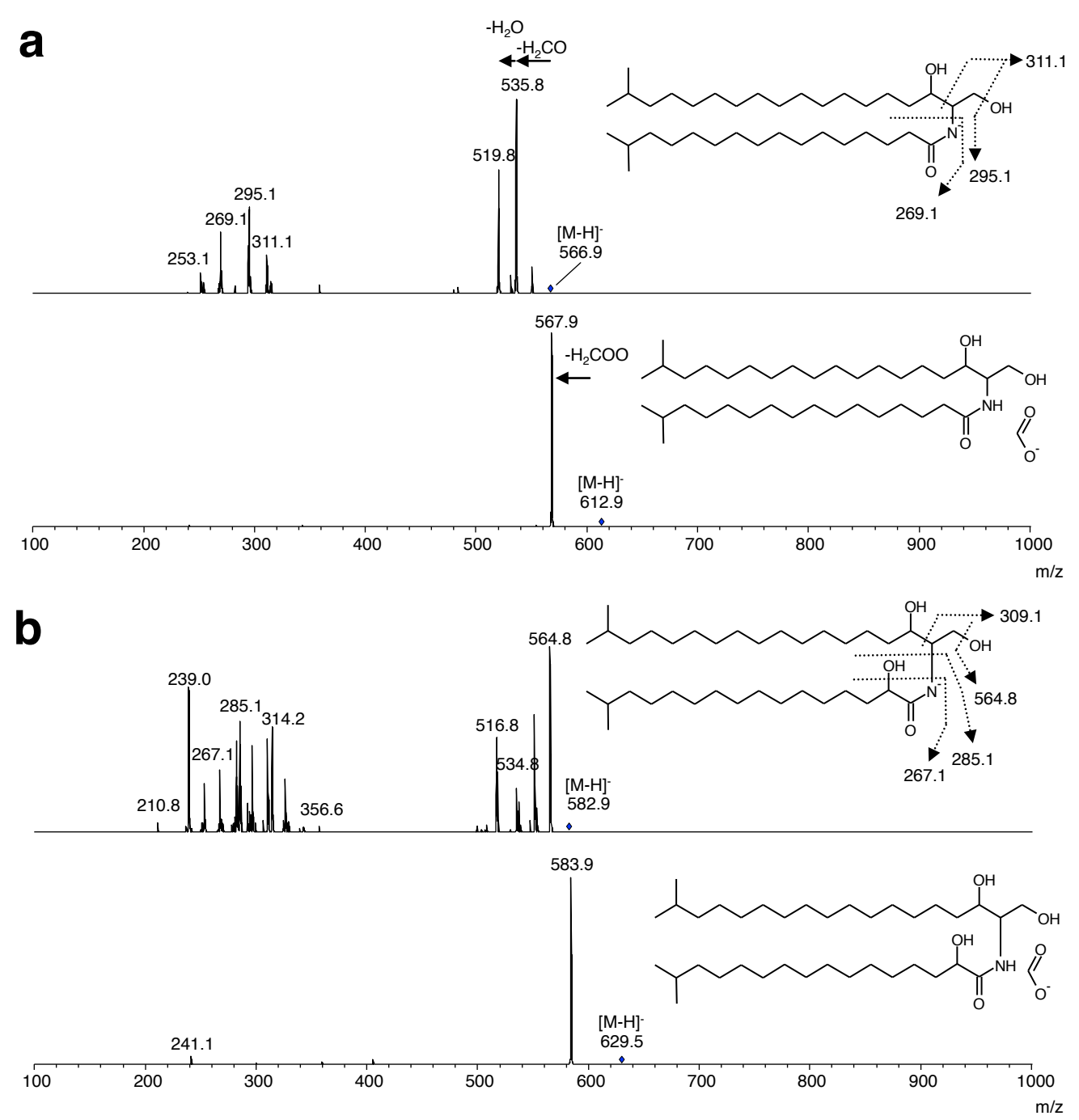

Supplementary Figure 4 | Example spectra for N-aclysphinganine (Cer) identification. Mass spectra of **a)** Cer(d19:0/17:0) and **b)** Cer(d19:0/17:0 2-OH). Structure elucidation was performed according to (50). The top spectrum was obtained from the $[M-H]^-$ and the bottom spectrum from the $[M+HCOO]^-$ molecular ion. Molecular composition was confirmed using hrMS (see Table 3).

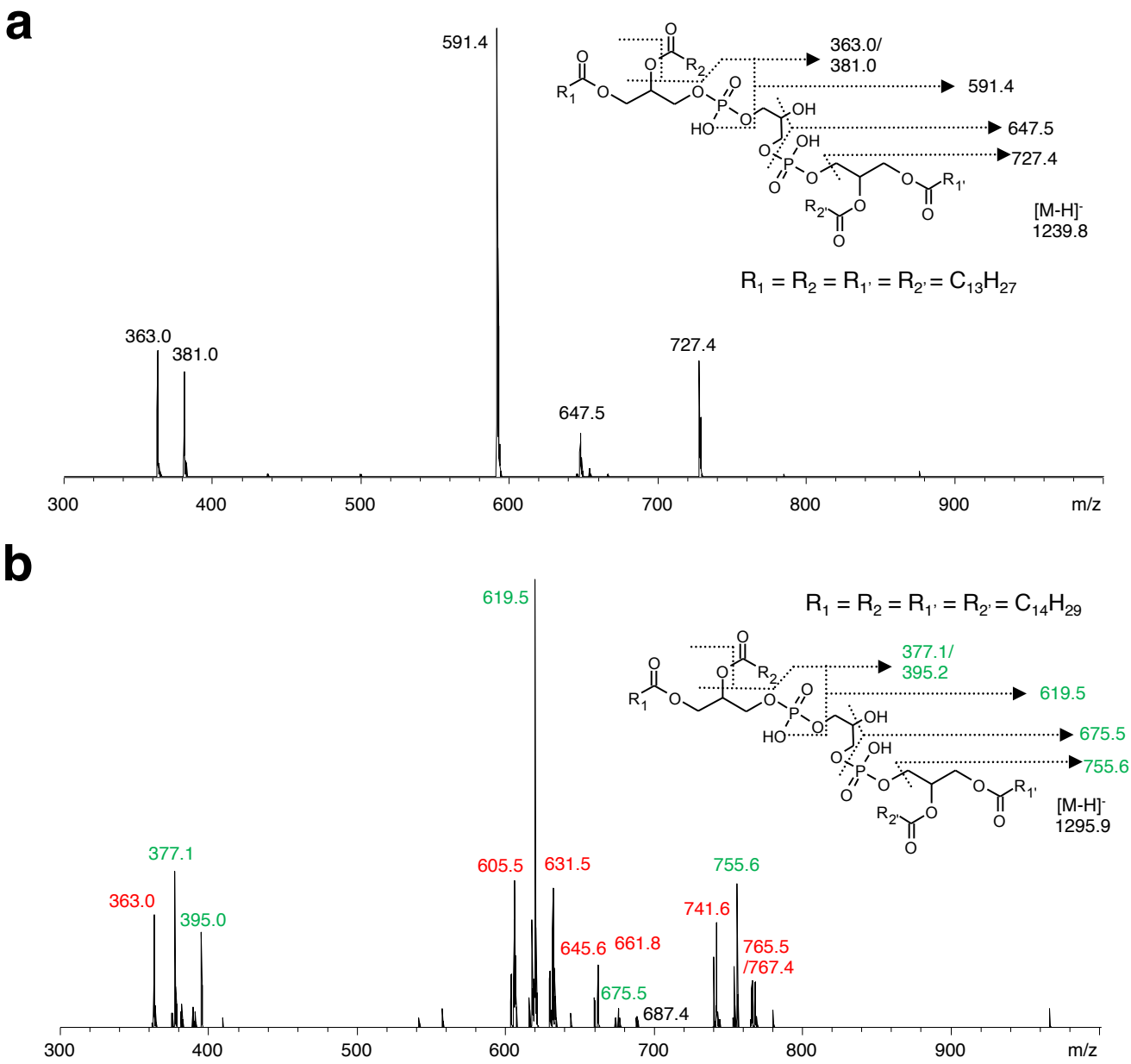

Supplementary Figure 5 | Example spectra for glycerophosphoglycerophosphoglycerol (Cardiolipin, CL) identification. MS^2 fragment spectra of **a)** CL(1'-[14:0/14:0],3'-[14:0/14:0]) standard and **b)** putative CL(60:0). Fragments are $[PA+131]^-$, $[PG-H_2O]^-$, $[IPA]^-$ and $[IPA-H_2O]^-$ (26). Fragments with green numbers in **b)** derive from CL(1'-[15:0/15:0],3'-[15:0/15:0]) and those in red from isotopic overlap with CL(60:2) (28).

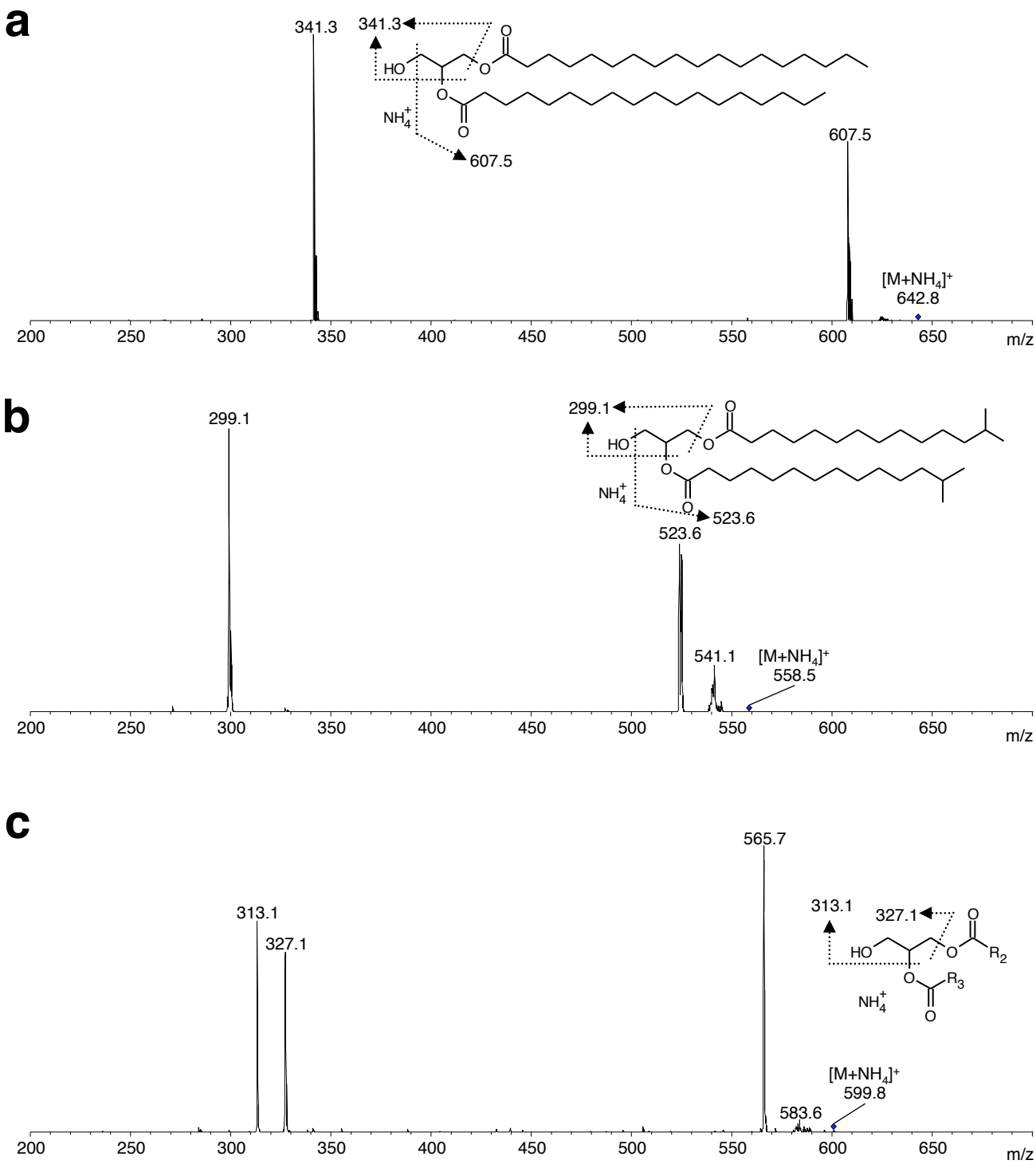

Supplementary Figure 6 | Example spectra for diacylglycerol (DG) identification. MS^2 fragment spectra of **a)** DG(18:0/18:0) standard **b)** DG(15:0/15:0) and **c)** DG(33:0) from $[M+NH_4]^+$ molecular ion. Fragment ions derive from neutral loss of fatty acid derived ketene moieties and water $[M-NH_3-H_2O-RCHCO]^+$ (37).

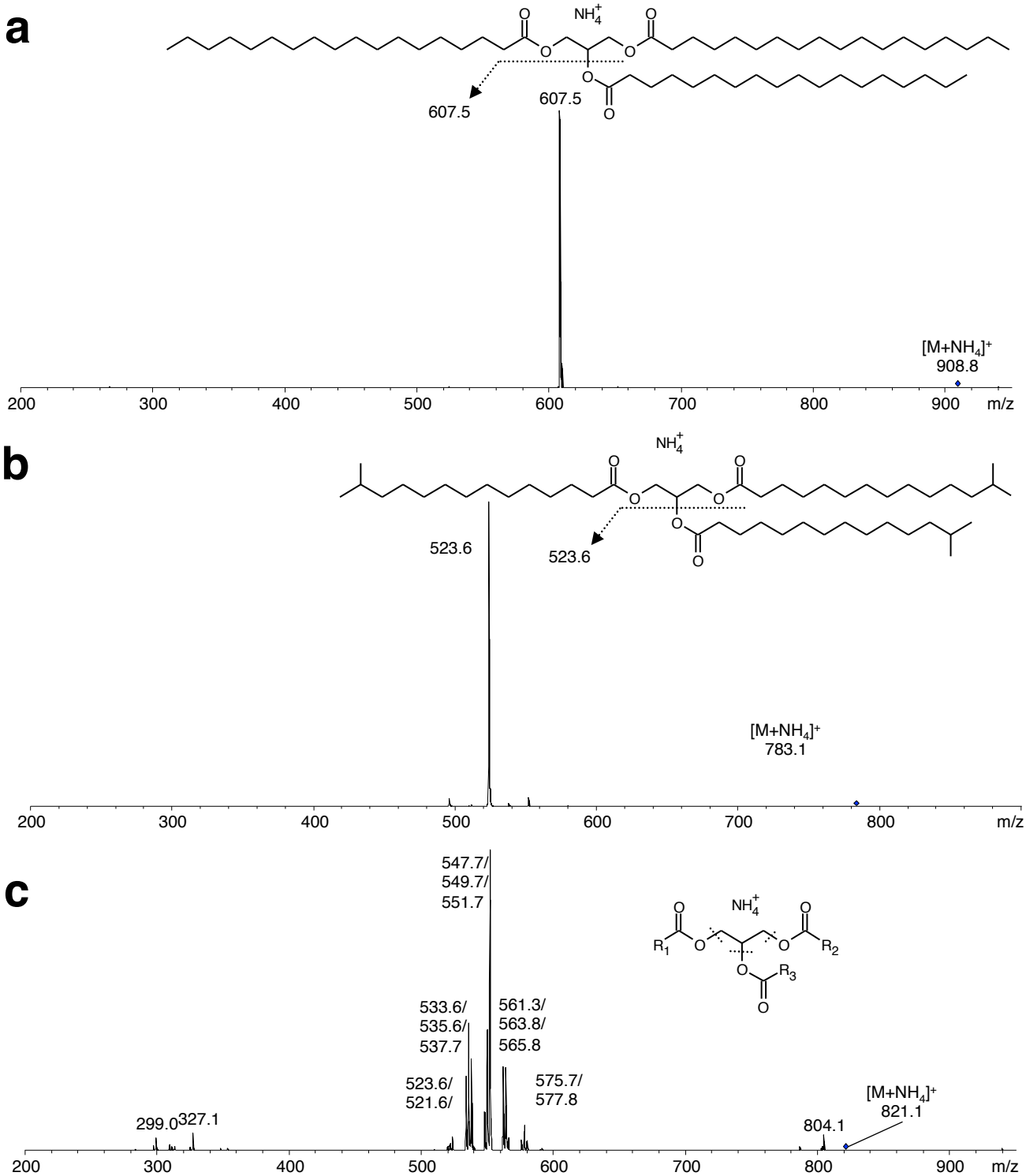

Supplementary Figure 7 | Example spectra for triacylglycerol (TG) identification. MS^2 fragment spectra of **a)** TG(18:0/18:0/18:0) standard **b)** TG(15:0/15:0/15:0) and **c)** TG(48:3) from $[M+NH_4]^+$ molecular ion. Fragment ions derive from neutral loss of fatty acids and ammonia ($[M-NH_3-R_nCOOH]^+$) (corresponding to fatty acids C14:1 to C18:2) and fatty acid derived $[R_nCO + 74]^+$ ions (37). The exact assignment of fatty acyl residues to glycerol backbone was not possible under these conditions.

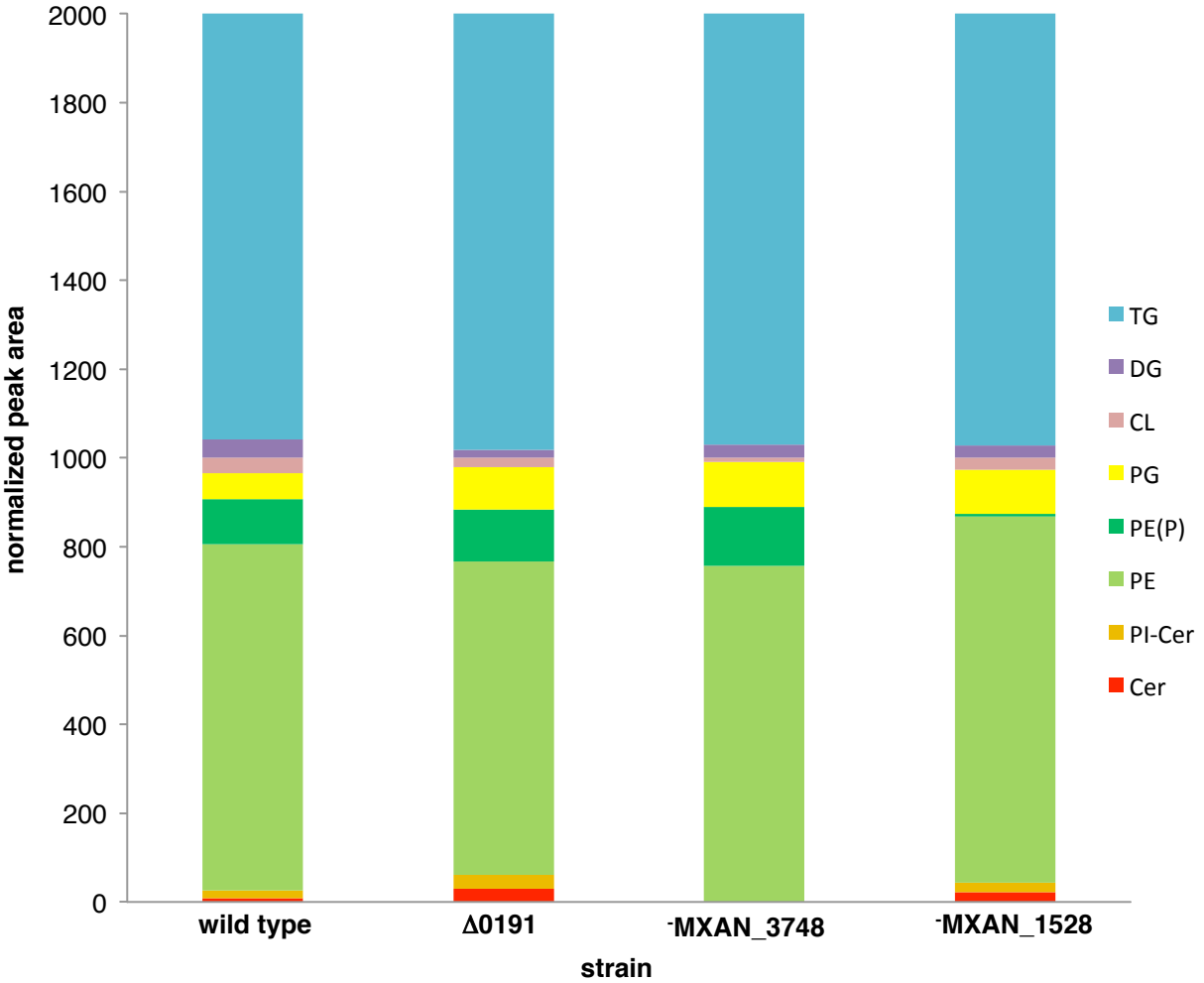

Supplementary Figure 8 | Ratio of lipid species present in lipid extracts. Ratios of lipid species present in various strains of *M. xanthus* given in per mil of total lipid AUC determined for the DG and TG in the positive and all other lipid species in the negative ionisation mode. TG: triacylglycerols; DG: diacylglycerols; CL: glycerophosphoglycerophosphoglycerols (cardiolipins); PG: glycerophosphoglycerols; PE(P): 1*Z*-alkenylglycerophosphoethanolamines; PE: glycerophospho-ethanolamines; PI-Cer: ceramide phosphoinositols; Cer: N-acylsphinganines.